Original Article

# DEVELOPMENT AND CHARACTERIZATION OF GEL-FORMING COMPOSITE FILM FOR OCULAR DELIVERY OF ACETAZOLAMIDE

**Fulchan Ali[1], Sk Habibullah[2,3], Swayongprava Behera[3], Satyajit Panda[3], Cahndrasekher Barik[3], Biswaranjan Mohanty[3*]**

[1]Research Scholar, Biju Patnaik University of Technology, Rourkela, Odisha, India.

[2]Department of Pharmaceutics, School of Pharmaceutical Sciences, Siksha 'O' Anusandhan (Deemed to be) University, Bhubaneswar-751003, Odisha, India.

[3]Department of Pharmaceutics, Institute of Pharmacy and Technology, Salipur, Cuttack, 754202, Odisha, India.

Email: biswaranjanm5@gmail.com

**DOI:** 10.47750/pnr.2022.13.S06.039

## Abstract

This work focus on the development of composite films of PVA (Polyvinyl alcohol) with different polysaccharides, Acetazolamide-loaded composite films were fabricated by solvent casting method. The developed films were characterized for weight uniformity, surface pH, thickness, gelling time, gelling capacity, % hemolysis, transparency study, mechanical study, FTIR analysis, impedance analysis, invitro drug release, ex vivo drug permeation, and ocular irritation study. The prepared films were colorless and clear. FTIR study revealed that no interaction between polymers. According to the stress relaxation investigation, the polysaccharide reinforced the PVA films and reduced their elastic component, Additionally, the residual elastic energy (P0) of the polysaccharide-loaded films was much greater than F0. The percentage hemolysis of all films was less than 5%, indicating highly compatible. The ocular tissue was not irritated by the synthesized composite film, confirmed by the Draize eye irritation test. Ex vivo transcorneal permeation of acetazolamide followed non-fickian diffusion process except F4.

**Keywords**: Acetazolamide, In-Situ film, Dissolution time, Regulated release, Residual elastic energy.

## 1. INTRODUCTION

The major disadvantage associated with ocular delivery was achieving minimal concentration in the site of action, which is a significant challenge for a researcher to overcome from the barrier. Tear generation, nonproductive absorption, transitory residence duration, and corneal epithelial impermeability mainly contribute to the poor bioavailability of the drug [1]. Degeneration of retinal ganglion cells was characterized by tunnel vision, the most prevalent eye disease and a leading cause of permanent blindness, otherwise known as glaucoma [2], which affects nearly 67 million people globally by increasing intraocular pressure (IOP) of the eye [3]. The carbonic anhydrase inhibitor acetazolamide (ACZ) lowers IOP in glaucoma sufferers. Low aqueous solubility and limited corneal penetration is the characteristic of ACZ [4]. As ACZ was a BCS class IV drug, by increasing the residence time increase in the therapeutic effect may be achieved.

Combining architectures of polymer and base with or without plasticizers is defined as a polymeric film, which is thin and flexible [5]. To over from that problem in the last few decades, film-type drug delivery, mainly in-situ film-type drug delivery, was attracting the researcher in comparison to the traditional dosage form because of its ease of use, low cost of Preparation, accessible transportation, and excellent patient compliance. Film-based drug delivery systems (FDDS) also deliver medicaments through buccal [6], ocular [7, 8], transdermal [9], and sublingual [10] channels to improve the therapeutic effectiveness and, as a result, decrease drug frequency. In-situ drug delivery is a new type of dosage form in which contact of film with the simulated tear fluid (STF) converts it into a thin gel-type ocuserts and releases the medicaments. Researchers have lately been interested in using polysaccharides to build mechanically and thermally improved composite film systems. Xanthan gum [11], sodium alginate [12], gellan gum [13], and pectin [14] are widely used polysaccharides for drug delivery applications.

In addition, polysaccharides were utilized as reinforcing material for preparing a composite film due to their natural abundance, cheap cost, non-toxicity, and low water vapor permeability [15].

Polyvinyl alcohol (PVA) is semi-crystalline and obtained from the polyvinyl acetate breakdown [16]. PVA is not only restricted to drug delivery [17] but also has a wide application in the field of food packaging [18], textiles [19], tissue engineering [20], and wound healing [21]. The distinctive properties of PVA are simple chemical structure, high swelling degree, water-solubility, non-toxicity, bioadhesive property, biocompatibility, non-inert, and elasticity, making it versatile. The biodegradability of PVA depends upon the quantity of hydroxyl group present in the polymer's backbone. The more the -OH group, the degradable nature, and vice versa [22, 23]. Nowadays, PVA was explored in new areas of research, such as glues [24], fibers [25], and hydrogels [26, 27]. PVA also has outstanding film-forming capabilities. PVA is non-toxic, odorless, transparent, flexible, and biodegradable when placed in environmental conditions [28], [29], [30]. It increases the mechanical strength of the film reported by various authors [5].

The pharmaceutical industry has widely used polysaccharides due to non-toxic, biodegradable, and stabilized self-life of the product. Rather than these polysaccharides were extensively exploited for their anti-tumor, immunomodulatory, antibacterial, antioxidant, anticoagulant, antidiabetic, antiviral, and hypoglycemic effects, make them most promising prospects in the biological and pharmaceutical industries Xanthan Gum (XG) was one of the polysaccharides most widely used as a dispersing agent and emulsion stabilizer in aqueous solutions owing to its rheological characteristics [31, 32] due to its unique attributes as non-toxic and safe for biological medium makes a choice of polymer in the food and pharmaceutical industry. In ocular drug delivery XG acts as a mucoadhesive polymer, which increases the residence of drug and improve the permeation rate. Gellan Gum (GG), obtained from the Pseudomonus eloda during aerobic fermentation, was widely used for sustained release drug delivery applications [33]. The extended residence duration on the corneal surface made it suitable to use in ocular drug delivery, and its ability to convert to gel in the ocular environment has previously been established [34]. Pectin has been used effectively in the food and pharmaceutical sectors for many years and was considered to be safe for human being. It has been employed as a mucoadhesive polymer for regulated medication administration because of its abundance in carboxylic groups and has the potential to interact with functional groups in the mucus layer (mucins). Instead, the potential for the formation of gels in acidic circumstances lengthens the contact duration of medications for ocular therapies [35]. Alginate is a linear unbranched polysaccharide obtained from brown algae and has a broad application area. Sodium alginate (SA) is a nontoxic, biopolymer with the capacity to gel at certain pH levels. The formation of the high viscosity acid gel is due to intermolecular binding and hydration of the alginic acid [36]. It was mainly used in the food and pharmaceutical industry [37] as a tablet disintegrator and gelling agent in ocular delivery [38].

As per the above finding, we aimed to formulate a novel acetazolamide thin film that has been prepared with the various type of polysaccharides. Best of our knowledge, no research has been explored in the area. The physicochemical property was characterized using spectroscopy (UV-Visible and FTIR), Dissolution time, mechanical, and electrical analyses. The in-vitro drug diffusion study was performed to release the drug acetazolamide. Ex-vivo permeation study was done to know the ocular permeability.

## 2. Material and Methods

### 2.1 Animal

IAEC (Institutional animal ethical committee) approved the experiment with protocol no 49/IAEC/IPT/19, dated 16/03/2019. The guideline of the Committee for control and Supervision of Experiments on Animals (CPCSEA), India, was followed [ Institution registration number: 1053/PO/RE/S/07/CPCSEA]. Animals were kept in the animal house of the Institute of Pharmacy & Technology, Salipur, Cuttack. The study was conducted using six white New Zealand rabbits (Oryctolagus cuniculus,1.6-2.2 kg), free from ocular disease.

### 2.2 Materials

PVA was purchased from Himedia (Mumbai, India). XG was purchased from Loba chemical (Colaba, Mumbai, India). GG was purchased from (Santacruz East, Mumbai, India), SA, and pectin was purchased from SRL Chemicals (Andheri, Mumbai, India). For the Preparation of STF analytical grade of NaCl, NaOH is used. Double distilled water is used throughout the experiment.

2.3 Method of Preparation

10% (w/w) PVA was weight and dissolved in 90.0 g of preservative water (composition: 0.2% of methylparaben & 0.02% of propylparaben) for a whole night. The mixture was homogenized using the magnetic stirrer for 3hr (600 rpm). In the same procedure, 1% (w/w) of GG, 1% (w/w) of pectin, and 1% (w/w) of XG were mixed with 99.0 g of preservative water to prepare the 1% solution, and 2% (w/w) of SA was incorporated in the 98.0 g of the preservative water to prepare the 2% SA solution. The polysaccharide solution was mixed using a magnetic stirrer having an rpm of 700 for 2 hr. then, the PVA solution (18.0g) and the different polysaccharide solutions (2.0 g) were homogenized together for 20 min using the over-head stirrer (700 rpm). 20 ml of water was then added to this suspension and homogenized for 10 min. Then the prepared mixture was sonicated for 30 min to remove the formation of a bubble. Again, the mixture was stirred for about 15 min using a magnetic stirrer at rpm 200. Then 10 ml of the mixture was measured through a measuring cylinder and poured into a Petri dish (diameter: 7.8 cm). Then the Petri dish was incubated at 400C for 24 h. for further analysis. The films were preserved in the air-tied zipper pouch at room temperature. The film prepared using only PVA is referred to as negative control. 100 mg of the acetazolamide drug was added before adding the polysaccharide solution. The drug-loaded films are F0D, F1D, F2D, F3D, F4D, and F5D. The composition of the prepared formulation was tabulated in Table 1.

2.4 Uniformity of weight & Folding Adherence

The prepared composite films were weighed by using a three-digit digital balance. The tests were carried out for each formulation in triplets. 2 cm X 2 cm of films are cut into squares and folded in the same places until the films break. The number of times the polymeric film has folded is the value of the folding adherence.

2.5 Thickness & Surface pH

The thickness of the prepared films was measured using the micrometer (Mitutoyo, Japan). The films were placed in between the upper and lower part of the micrometer, and the thickness was measured. The pH of the formulations was measured with a digital ATC pH meter (L1617 Elico Instrument Mumbai, India) at room temperature. Prepared film formulations are kept in contact with 2 ml of double-distilled water for 15 min and allowed to swell. Then the electrode was placed in the solution for 1 min without disturbance, and pH was recorded [39].

2.6 Determination of Gellation Time & Gellation Capacity

Gelation time was measured by Fathalla et al. [40] with slight modification. A small piece of film (1 CM X 1CM) was put on the watch glass containing STF (0.68 g sodium chloride, 0.2 g sodium bicarbonate, 8 mg sodium chloride dehydrate, and water to 1000 ml) at room temperature. The time in which the film is converted to the gel is noted down, and the final gellation time was recorded. It is a process in which, after the administration of the film into the route of administration, how quickly the patch is converted to gel to how long it would be in the unchanged condition is known as the gelling capacity determination. It can be calculated by the following method

– There was no gelation

+ The gel formed after a few minutes and quickly dissolved

++ The gel formed instantly and lasted for a few hours

+++ The gel formed quickly and remained stable for an extended period.

2.7 Hemocompatibility Test

Hemolysis of the prepared film was measured by Shah et al. [41]. Percentage hemolysis was calculated by using the below formula:

$$\%\ Hemolysis = \frac{OD\ test - OD\ negative}{OD\ positive - OD\ negative}\ X\ 100 \qquad (1)$$

2.8 Transparency study

Reading the numbers on a standard measuring ruler through the films allowed us to assess the films' clarity and transparency visually. Then, by taking a digital shot and comparing it to the measuring ruler, the proof of clarity was documented.

The developed films were measured for transparency using a UV-vis spectrophotometer (UV-1900i, Shimadzu Corporation, Duisburg, Germany). The PVA film was used as a control to adjust the spectrometer for the baseline correction. Films with a rectangular form (50 mm X 10 mm) were placed within the cuvette holder of the spectrophotometer and % transmittance (%T) was recorded in the range of 280–900 nm.

2.9 FTIR Study

Prepared in situ films were analyzed by attenuated total reflection infrared (ATR-IR) spectrometer (Alpha E ATR-FTIR, Bruker, USA) in the range of 4000–450 cm-1. This instrument was used to examine the chemical interaction between the in-situ gels. An average of 36 scans was reported [42].

2.10 Stress Relaxation Study

Mechanical properties of the prepared film were calculated from the stress relaxation study (SR) by using a static mechanical tester (TA_HD plus, Stable Micro System, Haskmere, England). The film samples were sliced into little rectangular pieces with a 50 mm 10 mm size. Following that, the samples were placed on sample holders with a sample length of 40 mm for the analysis. After that, the produced film samples were stretched at a rate of 1 mm/sec to a distance of 1 mm. The probe was maintained in the same place for 60 seconds to enable the tension in the film to release.

$$\% SR = \frac{F0-F60}{F0} X\ 100 \qquad (2)$$

$$\mathrm{P(t)} = \mathrm{P_0} + \mathrm{P_1} \times \mathrm{e}^{\frac{-\mathrm{t}}{\tau 1}} + \mathrm{P_2} \times \mathrm{e}^{\frac{-\mathrm{t}}{\tau 2}} \qquad (3)$$

A pair of grips on the AT/G probe was attached with film strips measuring 1 cm by 4 cm. Initial grip separation was set at 50 mm, and cross-head speed was set to 1 mm/s.

The maximum load (N) was divided by the cross-sectional area to get the TS:

$$TS\ (MPa) = \frac{Breaking\ Load\ (N)}{Cross\ Sectional\ area\ of\ the\ Sample} \qquad (4)$$

2.11 Impedance Analysis

A computer-controlled impedance analyzer was used to determine the conductivity profile of the formulated gel product (Phase-sensitive multimeter, PSM1735, Numetriq, Japan). At ambient temperature, the experimental results were collected as a function of frequency (0.1Hz-1MHz).

2.12 In vitro drug diffusion time

Modified Franz diffusion cell was used for the release of the drug using a semipermeable membrane ( molecular weight cutoff 65kDa). A small piece of film (1 cm2) was placed on a semipermeable membrane and fixed between the receptor and donor compartment. The receptor compartment containing 12 ml of STF and the temperature was maintained at 370 C [42]. 1 ml of samples were withdrawn at fixed interval of time and same volume was replaced with STF. The collected samples were analyzed for drug content at 267 nm using uv-visible spectrophotometer. [43].

2.13 Ex-vivo drug diffusion study

To know the permeation behavior of drugs in the eye, a permeation study was done using freshly excised goat cornea. The study was done through the modified Franz diffusion cell having a diffusion area of 1.54 cm2. The experiment was conducted for 3hr.

2.14 Eye irritation test

For ophthalmic preparations, the Draize eye irritation test is the most often used test. This test is used to investigate the ophthalmic preparations' safety and toxicity [44]. As a consequence, the developed film formulation was tested for eye irritation using the Draize method to check whether it was acceptable for use as an ophthalmic treatment. The experiment included injecting prepared film into the cul-de-sac and monitoring it for the next 72 hours.

## 3. Result and Discussion

3.1 Visual Appearance and Transparency

All the films are found to be transparent because they contain a high amount of PVA which makes them colorless (Figure 1a-e). The films are prepared by solvent casting method which is a cheap and easy process to prepare the film. Yadav et, al also prepared a film by using PVA which is cytocompatibility with mammalian cells. They also found that prepared films are transparent [45]. All the prepared films were smooth. Among all the formulations blank film (F0) is very smooth and transparent with compare to others.

3.2 Uniformity of Weight and pH

The weight and the pH of the films were tabulated in Table 2. The weight of the films were varied between 0.683 ± 0.013 to 0.754 ± 0.024 (mg). All the formulation pH ranges from 6.71 to 7.09, which indicates that the formulation does not cause any type of irritation or swelling to the eye.

3.3 Thickness and Folding Adherence

The thickness of the films were varied from 84.5 ± 0.3 to 106.36 ± 0.45, and folding adherence of all the film was found to be greater than 100 (Table 2). It was reported that the value of folding endurance of less than 200 has provided enough strength and durability for the films [46].

3.4 Determination of Gellation time and Gellation Capacity

The gelation period was essential in in-situ formulations because it influences drug release at the site of action. The formulas' gelation times range from 19 to 38 seconds (Table 2). Because it took longer to slide, the inclusion of acetazolamide (a medication that is insoluble in water) had a significant influence on the sol dynamics. All the composite films f had a "+++" gelling capacity, indicating that they gelled swiftly and stayed in the same condition for an extended period of time, making the formulation more patient-friendlier.

3.5 Hemocompatibility Test

The hemocompatibility tests used in this study were mostly based on the ASTM standard [47]. According to the author [48], if the hemolysis percentage is less than 5%, then it is highly compactable. In our study, we found that all the formulations were highly compatible, and the result is tabulated in table 2.

3.6 Light Transmission Study

Reading the numbers on a ruler that was maintained beneath the films allowed for visual evaluation of the transparency of the films (Figure 2a-e). In every picture, it was simple to read the numbers on the ruler. All the film formulations were transparent

in nature. The films' transparency was further examined by UV-visible spectroscopy. Figure 3 shows UV-visible wavelength spectra from 280 to 900 nanometers. Low UV-visible transmittance was evident in the control film (F0). UVB, UVA, and visible ranges are the wavelength ranges between 280 and 320 nm, 320 to 400 nm, and 400 to 700 nm, respectively [49].

The percentage transmittance of the pure PVA film was 56.81 in the UVB region. The average percent transparency of the UVB films was reduced by incorporating the polysaccharide content. The average transmittance was found to be in a order of F1 > F2 >> F3> F4 for 41.11,40.12,32.91, 30.77 respectively.

The overall percentage transparency of both control and polysaccharide-containing films significantly changed in the UVA area. The control film's average percent transmittance was measured at 81.44 percent, which was greater than the film's average percent transparency in the UVB zone. Additionally, the average percent transparency of films containing polysaccharides was raised to 81.25 (F1), 80.49 (F2), 72.98 (F3), and 75.03 (F4). It should be mentioned that UV rays with wavelengths between 290 and 350 nm are the most dangerous to human health [50]. In phase-separated films made of hydroxypropyl methylcellulose and hydroxypropyl starch, a similar discovery of a polysaccharide's (pectin) reduction in transparency in the UV region has been observed [51].

There were minor changes in the control film's transmittance spectra in the visible region (400 nm–700 nm). The average % transparency of F0 was 88.87. In comparison to the control film, the polysaccharide-containing films had increased average percent transparency. The average percentage transmittance of F1, F2, and F4 was nearly significant. The overall transparency was 87.37, 87.43, and 84.54, respectively. Polysaccharides containing formulation F3 show 81.70 percent transmittance. From 400 nm to 700 nm, the average percent transparency of films F0-F2 was nearly 90%, which is regarded as the optimal criterion for hydrogel films in biomedical applications [52].

### 3.7 FTIR Study

The FTIR analysis was carried out to know the interaction between the excipient and the polymer base (i.e., polyvinyl alcohol). A broad spectrum was observed in all the formulations shown between 3730 cm-1 to 3001 cm-1 in Figure 4 (a-e). Common signals are found in all formulation are 2941 cm-1, 1430 cm-1, 1086 cm-1 1727 cm-1, 1249 cm-1, 840 cm-1. The broadness in the formulation was due to the increase in the hydrogen bonding in the formulations and indicates the hydrogen bonding interaction between O-H group of polysaccharides and PVA. A common peaks 2941 cm-1 was found in all formulation except F2, which indicates the C-H stretching [53]. The peak at 2932 cm-1 in F2 was attributed to the C-H stretching vibration [54]. A common peak of 1727 cm-1 was found in all the formulations, which indicate the C=O stretching vibration peak [55]. The peak 840 cm-1 was responsible for the α-linkage of a glycoside. The peak of 1086 is attributed mainly to the hydrogen bond interaction between the primary and secondary alcohol groups [56].

We can co-relate the AUP with the gelling time. The strength of the hydrogen bond binding interaction has a significant impact on both the entrapment and release of solutes [57]. As the hydrogen bond was increases it entraps the water molecule, and contact with the polysaccharide to form hydrogel, which is known as gelation time. More the hydrogen bond less the gelling time was noted. It was descript in the figure 5.

### 3.8 Stress relaxation Parameter

The mechanical property of the prepared film was evaluated using a stress relaxation study. It was conducted in the extension mode. The viscoelastic profile are shown in figure 6a. The force values measured by the probe rose as the films were stretched, eventually reaching a peak value (F0) at the completion of the stretching period (Figure 6b). The probe was kept in place at this stage, and the films were allowed to relax. The force levels fell rapidly as time passed throughout the relaxing period. At the conclusion of the relaxation period, the force values reached a minimal constant level (F60) (Figure 6c). The F0 value of F4 was the lowest among the all prepared film and F0 was highest in the prepared film, then there is a negligible difference between the F1 and F2 value. Also F0 film has the highest F60 value. It can be observed that the F60 value of F1, F2 and F4 is nearly same. F3 has the lowest F60 value. % SR was calculated by the Eq 2. The % SR value of the films have been utilized to gain information regarding the viscoelastic nature of the prepared sample. From the % SR it can be concluded that the nature of film is viscoelasticity or plasticity, where is in ideal fluid % SR value is obtained 100 is known that plasticity and 0% SR is known as elastic solid. % SR of the Formulation F1 and F2 is same where as in F4 it was slightly changed which is negligible. The % SR value in F3 was found to be lowest. To observed the viscoelastic behavior of the films, the normalized force vs. time profile (Figure 6d) graph was fitted to Weichert's model (Eq. 3). The modulus of elasticity (P0, P1, and P2), and modulus of viscosity (τ1 and τ2) of the films were determined by fitting the data to this model [58]. The fitted profile have been demonstrated in

(Figure 6f) while the parameter are tabulated in the table 3. All of the films' correlation coefficients between experimental and fitted data were more than 0.99. The leftover elastic energy at the conclusion of the relaxing phase inside the films is represented by the model parameter P0. The establishment of a repeatable and dependable network structure is indicated by high P0 values. The residual force value in F4 was found to be highest, which suggested that the it retained significantly more elastic energy as compared to others prepared films. The P0 value is low in F1 then it will be same in F2 and F3. Variations in instantaneous relaxation time (τ1) may be used to investigate the impact of stress on molecular rearrangement within formulations. F2 has the quickest relaxation time. The τ2 is known as the long duration relaxation time and aids in the analysis of polymer chain interaction breaking when stress is applied [59]. Here also F2 shows faster molecular breaking as compared to others. Then F3, F1, and F4 shows the molecular breaking in the composite film. Table 3 displays the outcomes for the assessments of tensile strength (TS) and SR for all film compositions. TS of F0 was found to be highest (3.379 Kg/mm2), then all the composite films were decreases as compare to the control. Lowest TS was found in case of F4 which was (2.112 Kg/mm2).

The decrease of the TS of the film may be due to the polysaccharide gum's OH group (water) likely decreased the film's stiffness and resistance to elastic force, which in turn decreased the composites TS, which was clearly seen in the modules of elasticity parameter (P0) [60].

3.9 Impedance Spectroscopy

To evaluate the electrical property of films they are subjected to the impedance analysis. It is one of the key tools for predicting the drug release profile from pharmaceutical formulations. Similarly, iontophoretic drug delivery techniques greatly depend on the electrical behavior of the formulations [49]. Addition of polysaccharide altered the electical properties of the composite films (Figure 7). Comparing with the control, the impedance of all films was decreased upon addition of polysaccharides except F1(gellan gum). The increased conductivity within the formulation could increase the drug release from the formulations.

3.10 In-Vitro Drug Release Study

Drug release study was conducted for 180 min, and result was shown in Figure 8a. The CPDR from F1 was the lowest. The film (F4) containing xanthan gum showed highest CPDR. The release profiles were modelled using the Korsmeyer-Peppas model (Figure 8b) in order to comprehend the intrinsic release features and result were tabulated in the table 4. The Korsmeyer-Peppas model (Eq. 5) suggested that the diffusion parameter (k) was decreased for F1 in compare to the control. Then in rest of the formulation k value was increased. Except for F4, diffusion exponent values (n) of all composite film were between 0.58 and 0.87. This suggests that the drug release was not mediated by Fickian diffusion and was instead caused by the interaction of the Fickian and polymer chain relaxation processes [61]. The n value for F4 was less than 0.45 which reflect the fickian diffusion of the drug [62]. The release data was again fitted to the Peppas-Sahlin (PS) model by using Eq. 6 (Figure 8c). This was used to compute the polymer relaxation constant (kr) and the Fickian diffusion constant (kd), which were shown in Table 4.The PS model parameter findings showed that the diffusion process from composite films was impacted by polymer relaxation.

$$C = k\, t^n \qquad (5)$$

Where C = cumulative percentage drug release, k = diffusion parameter, n= diffusion exponent.

$$F = k_d t^m + k_r t^{2m} \qquad (6)$$

where Kd is the constant related to the Fickian kinetics; Kr is the constant that is related to Case-II relaxation kinetics; m is the diffusional exponent which inhibits controlled release.

3.11 Corneal Permeation study

When developing an effective ocular drug delivery system, it is necessary to evaluate the permeation of the drug molecules over the cornea to the interior structures of the eye into account. A corneal permeation investigation was carried out using freshly excised goat cornea and the cumulative drug permeation (CPDP) profile was shown in Figure 8(d). For better under the CPDP data was fitted to the Korsmeyer-Peppas model and Peppas-Sahlin in equation 7 and equation. 8 respectively. The model parameters are shown in Table 5.

The Korsmeyer-Peppas model fitting revealed that the release exponent was less than 0.45 in F4. This is consistent with the medications' Fickian diffusion through the ocular tissue.

The Peppas-Sahlin model fitting, which estimated the Fickian diffusion constant (Kd) tabulated in the table 5. All formulations had a Kd/Kr ratio greater than 1, which further supported the Fickian transport-driven mechanism for moving drug molecules through ocular tissue.

$$F = K_c t^{n_c} \quad (7)$$

where F is the fraction of solute released; Kc is the release rate constant; t is the time of sampling and nc is the release exponent.

$$F = K_d t^m + K_r t^{2m} \quad (8)$$

where Kd is the Fickian diffusion constant; Kr is the polymer relaxation constant; m is the diffusional exponent that exhibits controlled release.

3.12 Eye irritation Study

To evaluated the study of eye irritation Draize test is commonly used. To know the safety and toxicity the test is required, and done in the aseptice condition [44]. So the prepared patch were subjected to the Draize eye irritation test to see whether it's suitable for ophthalmic preparations. In this study, the composite films were inserted into the cul-de-sac and monitored for 72 hours throughout the research. After 72 hours, there was no chemosis of the cornea or other ocular tissues, according to the findings. This suggested that the produced in-situ patch may be employed for ocular administration.

Table 1: Formulation Table of the in-situ patch

| **Formulations** | **PVA Solution (g)** | **Different types of gum used** | | | | **Acetazolamide (g)** | **Distilled Water (g)** |
|---|---|---|---|---|---|---|---|
| | | **Gellan Gum (1% w/v)** | **Pectin (1% w/v)** | **Sodium Alginate (2% w/v)** | **Xanthan Gum (1% w/v)** | | |
| **F0** | 20 | -- | -- | -- | -- | -- | 20 |
| **F1** | 18 | 2 | -- | -- | -- | -- | 20 |
| **F2** | 18 | -- | 2 | -- | -- | -- | 20 |
| **F3** | 18 | -- | -- | 2 | -- | -- | 20 |
| **F4** | 18 | -- | -- | -- | 2 | -- | 20 |
| **F0D** | 20 | -- | -- | -- | -- | 0.1 | 20 |
| **F1D** | 18 | 2 | -- | -- | -- | 0.1 | 20 |
| **F2D** | 18 | -- | 2 | -- | -- | 0.1 | 20 |
| **F3D** | 18 | -- | -- | 2 | -- | 0.1 | 20 |
| **F4D** | 18 | -- | -- | -- | 2 | 0.1 | 20 |

Table 2: Physicochemical Properties of the Ocular Film

| Formulation Code | Uniformity of Weight (mg) | pH | Thickness (µm) | Gelling time (sec) / Gelling capacity | % Hemolysis | Folding Adherence |
|---|---|---|---|---|---|---|
| F0 | 0.68 ± 0.00 | 6.8 ± 0.05 | 84.5 ± 0.3 | 19.33 ± 3.05 (+++) | 0.434 | > 100 |
| F1 | 0.68 ± 0.01 | 6.89 ± 0.07 | 90.93 ± 0.25 | 31.66 ± 3.51 (+++) | 0.178 | > 100 |
| F2 | 0.70 ± 0.00 | 6.71 ± 0.13 | 95.43 ± 0.47 | 38.66 ± 3.51 (+++) | 0.135 | > 100 |
| F3 | 0.75 ± 0.02 | 7.09 ± 0.09 | 102.56 ± 0.45 | 36.66 ± 3.05 (+++) | 0.114 | > 100 |
| F4 | 0.74 ± 0.03 | 6.88 ± 0.07 | 106.36 ± 0.45 | 37.33 ± 3.21 (+++) | 0.196 | > 100 |

Table 3: Mechanical Parameter of the Prepared film

| Model | Model Parameter | F0 | F1 | F2 | F3 | F4 |
|---|---|---|---|---|---|---|
| | **F0** | 1517.05 | 132.2953 | 128.7126 | 113.0548 | 91.16035 |
| | **F60** | 286.712 | 83.19875 | 81.87182 | 82.53528 | 57.32354 |
| | **%SR** | 81.1006 | 37.11133 | 36.39175 | 26.99533 | 37.1179 |
| | **TS (kg/mm$^2$)** | 3.37934 | 2.41429 | 3.01378 | 2.46046 | 2.1125 |
| **Weichert Model** | **P0** | 0.19299 | 0.629768 | 0.635365 | 0.72847 | 0.6304 |
| | **P1** | 0.52837 | 0.134756 | 0.138483 | 0.10327 | 0.13241 |
| | **T1** | 0.82961 | 15.0865 | 14.40138 | 15.3647 | 12.7147 |
| | **P2** | 0.27028 | 0.231703 | 0.223044 | 0.16385 | 0.23476 |
| | **T2** | 13.0066 | 0.767118 | 0.726381 | 0.78953 | 0.62583 |
| | **R2** | 0.9981 | 0.996955 | 0.996883 | 0.99631 | 0.99579 |

Table 4: Diffusion Model Parameter

| Model | Model Parameter | F0 | F1 | F2 | F3 | F4 |
|---|---|---|---|---|---|---|
| | k | 0.621661 | 0.589378 | 0.885668 | 0.953703 | 3.535859 |
| | n | 0.696836 | 0.696813 | 0.643486 | 0.640282 | 0.427297 |
| **KP Model** | R2 | 0.998123 | 0.998683 | 0.997449 | 0.996829 | 0.995108 |
| | Kd | 0.863922 | 0.81403 | 1.151714 | 1.231041 | 3.542949 |
| | Kr | 0.062995 | 0.073335 | 0.076648 | 0.094454 | 0.528472 |
| **PS Model** | Kd/Kr | 13.71409 | 11.10012 | 15.02603 | 13.03317 | 6.704132 |
| | m | 0.502692 | 0.489543 | 0.480764 | 0.470961 | 0.317759 |
| | R2 | 0.998975 | 0.999322 | 0.998182 | 0.997924 | 0.996218 |

Table 5: Permeation Model Parameter

| Model | Model Parameter | F0 | F1 | F2 | F3 | F4 |
|---|---|---|---|---|---|---|
| KP Model | $k_c$ | 0.050673 | 0.065752 | 0.094933 | 0.095082 | 0.417618 |
| | n | 0.765506 | 0.67912 | 0.652177 | 0.640495 | 0.396717 |
| | $R^2$ | 0.990883 | 0.998099 | 0.993928 | 0.99618 | 0.998157 |
| PS Model | Kd | 0.07587 | 0.089411 | 0.123817 | 0.122878 | 0.432093 |
| | Kr | 0.003606 | 0.006709 | 0.008013 | 0.009144 | 0.032629 |
| | Kd/Kr | 21.04214 | 13.32711 | 15.45216 | 13.43758 | 13.24257 |
| | m | 0.566546 | 0.49179 | 0.488221 | 0.472835 | 0.325214 |
| | $R^2$ | 0.993174 | 0.998829 | 0.99543 | 0.997179 | 0.998234 |

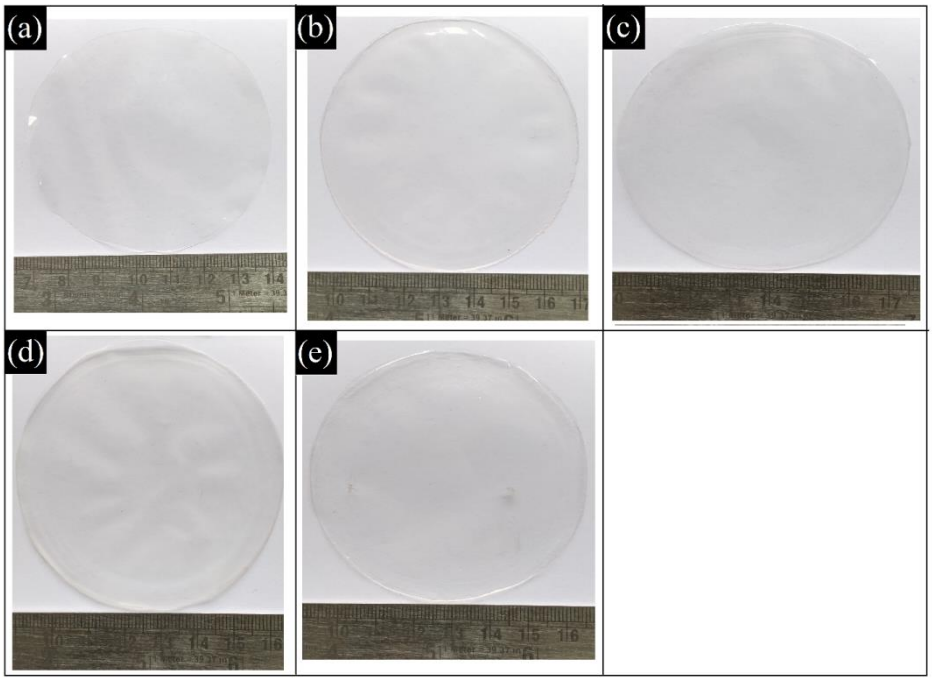


Figure 1: Photographic Image of Prepared composite film (a) F0, (b) F1, (c) F2, (d) F3, and (e) F4.

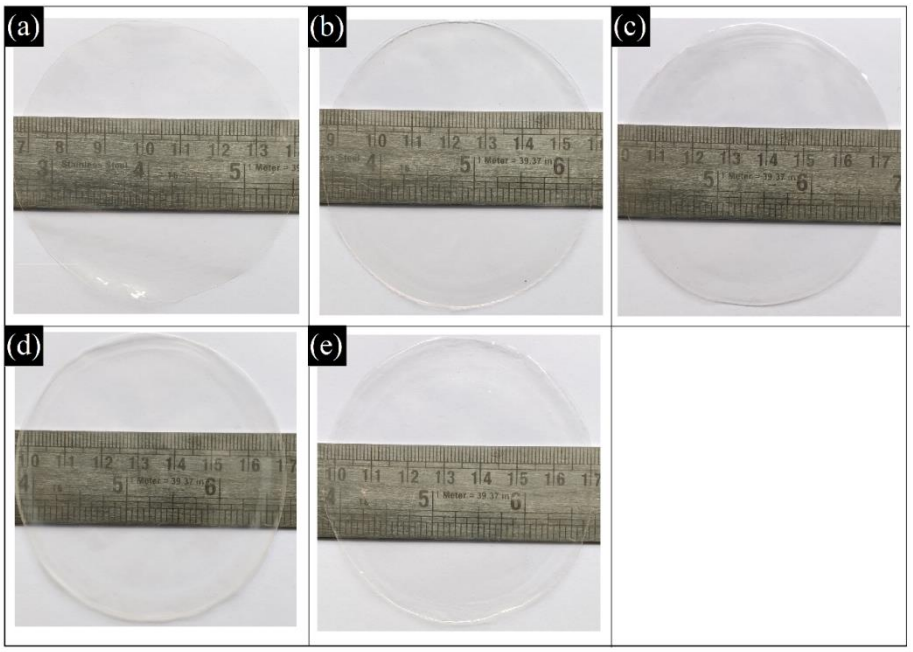


Figure 2: Transparency of composite film with ruler (a) F0, (b) F1, (c) F2, (d) F3, and (e) F4.

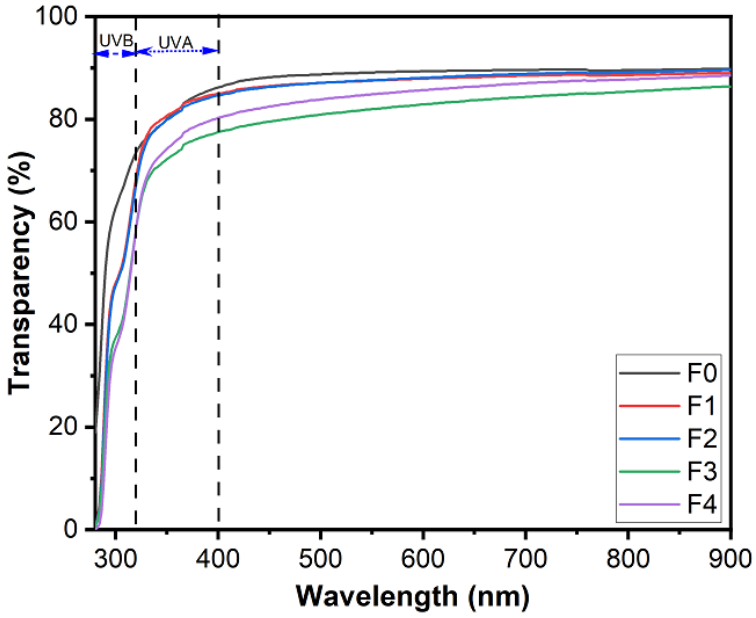


Figure 3: Transparency (%) of composite film (a) F0, (b) F1, (c) F2, (d) F3, and (e) F4.

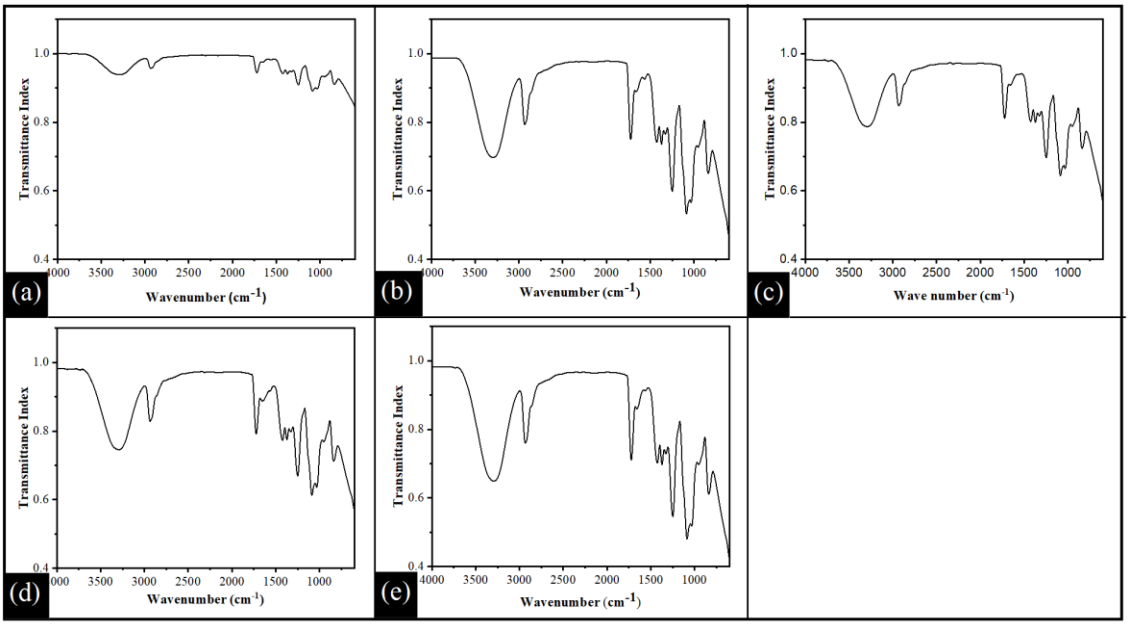


Figure 4. FTIR spectra of prepared In-situ Film (a) F0, (b) F1, (c) F2, (d) F3, (e) F4.

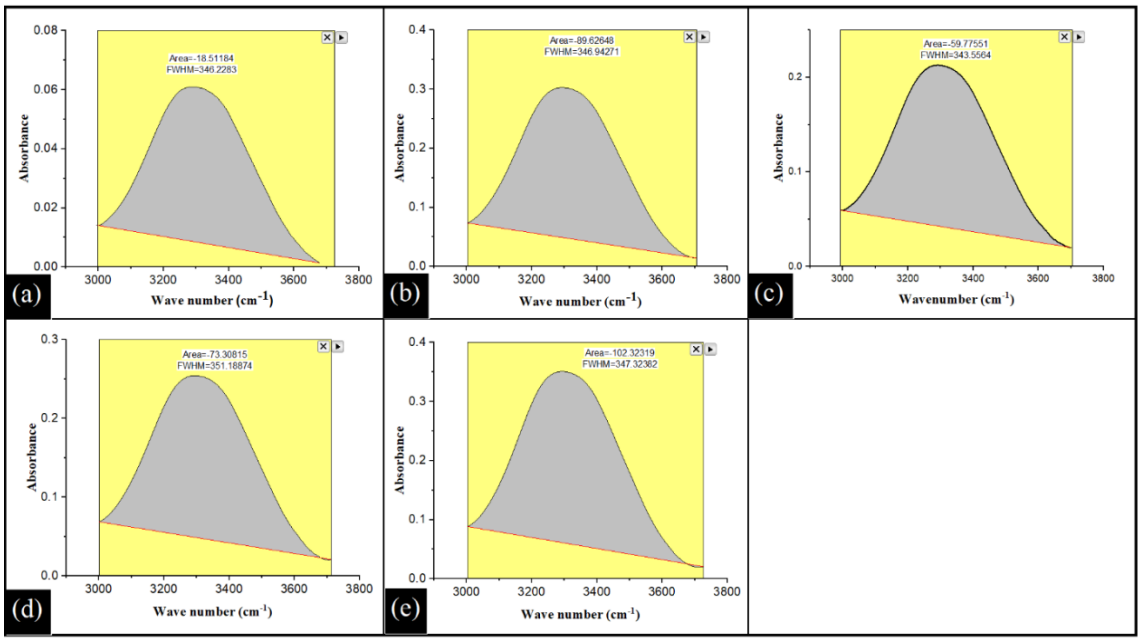


Figure 5; AUP of the prepared In-situ film (a) F0, (b) F1, (c) F2, (d) F3, (e) F4.

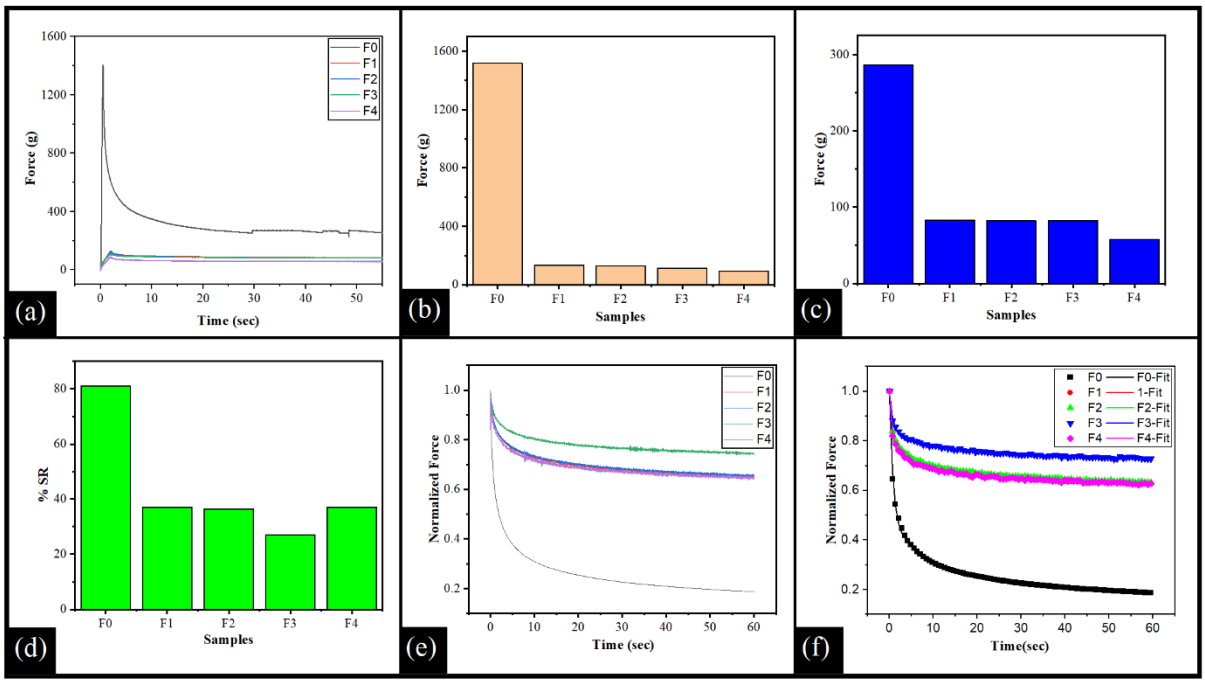


Figure 6: (a) Stress Relaxatation Profile, (b) F0, (c) F60, (d) %SR, (e) Normalized Force, (f) Wiechert model fitting.

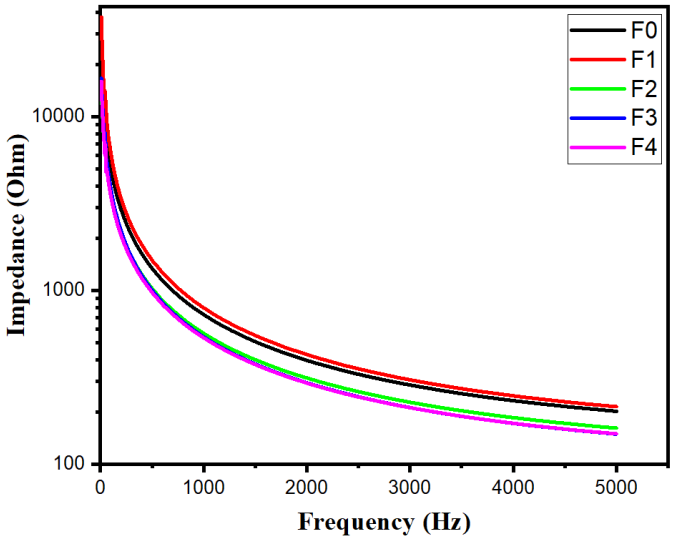


Figure 7. Impedance profile of the composite films.

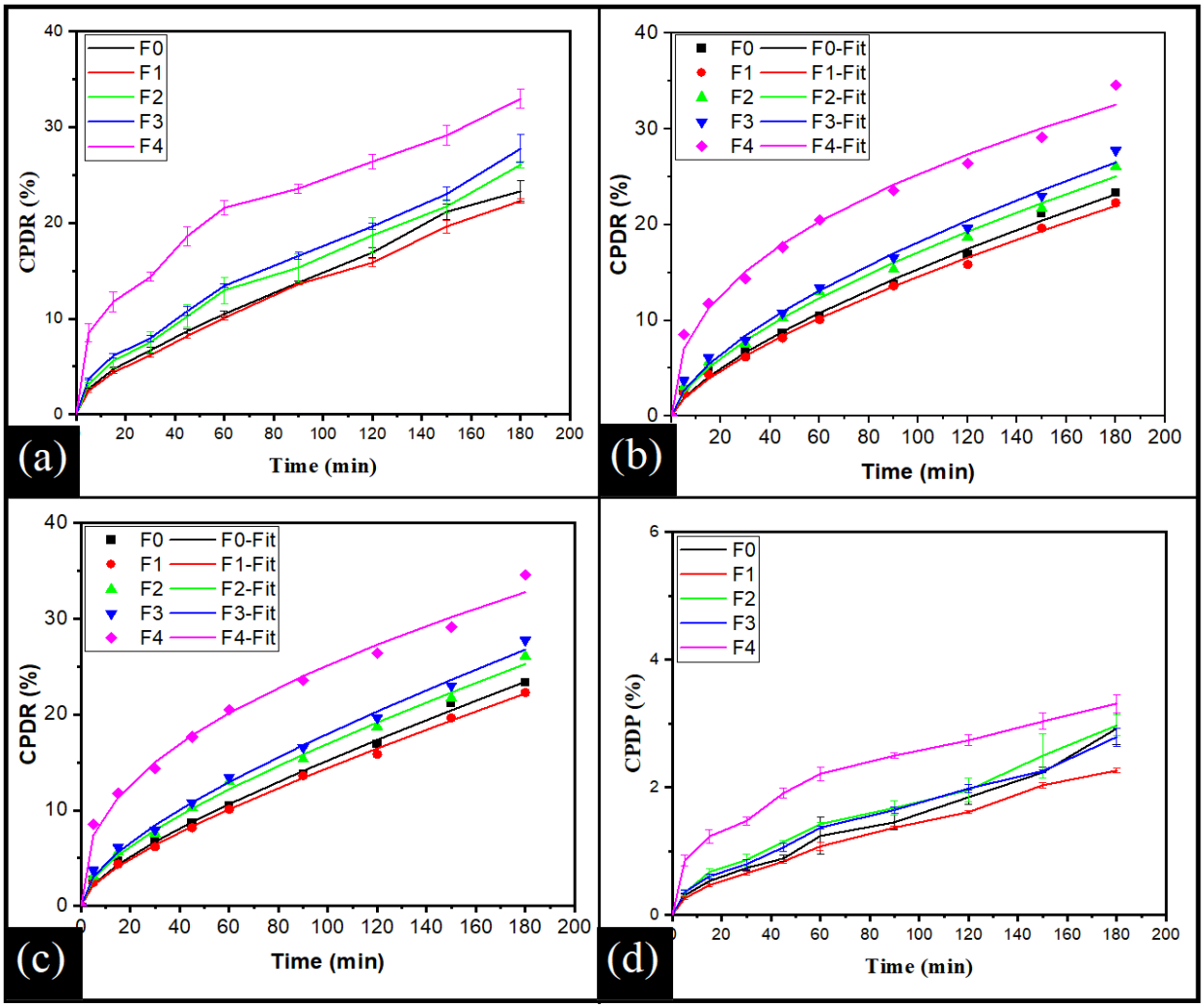


Figure 8: Drug release from the Prepared film (a) Diffusion, (b) Korsmeyer-Peppas model fitted to CPDR Profile, (c) Peppas-Sahlin model fitted to CPDR Profile (d) % CPDP Profile.

## Conclusion

In this work, we used the solvent casting method to formulate polymer composite films based on PVA with gellan gum, pectin, sodium alginate and xanthan gum. All physicochemical properties of the composite films indicated the ideal for ocular application. All the prepared films were appear to be smooth and clear. Films containing (F4) xanthan gum showed highest CPDP followed by F3 (sodium alginate) and F2 (pectin). The drug diffusion and permeation profile of all films showed non-fickian process except F4. Eye irritation study confirmed the safety for ocular application. The polysaccharide reinforced the PVA films and reduced their elastic component, according to the stress relaxation investigation. Additionally, the residual elastic energy (P0) of the polysaccharide loaded films was much greater than F0. The alteration of conductivity of the films were observed in impedance study. According to the above finding, the PVA/Polysaccharide based composite films could be suitable for ocular application.

Acknowledgement

Authos are thankful to Institute of Pharmacy and Technology, Salipur for providing facilities for this research work .

Author Contribution

Conceptualization: Biswaranjan Mohanty, Methodology: Fulchan Ali, Sk Habibullah, validation: Satyajit Panda and Swayongprava Behera, Investigation: Fulchan Ali, writing—original draft preparation: Fulchan Ali, Writing—review and editing: Sk Habibullah, Biswaranjan Mohanty, Supervision, project administration: Biswaranjan Mohanty. All authors have read and agreed to the published version of the manuscript.

Funding

No external funding for the research work.

Conflict of Intrest statement

The author declars that there is no conflict of intrest

Ethical Committee Approval

Institutional animal ethical approval was obtained for this investigation by license 49/IAEC/IPT/19, dated 16/03/2019.

## REFERENCES

1. Rathore, K., In situ gelling ophthalmic drug delivery system: an overview. Int J Pharm Sci, 2010. 2(4): p. 30-4.
2. Sun, J. and Z. Zhou, A novel ocular delivery of brinzolamide based on gellan gum: in vitro and in vivo evaluation. Drug design, development and therapy, 2018. 12: p. 383.
3. Kaur, I.P., H. Singh, and S. Kakkar, Newer therapeutic vistas for antiglaucoma medicines. Critical Reviews™ in Therapeutic Drug Carrier Systems, 2011. 28(2).
4. Mohsen, A.M., A. Salama, and A.A. Kassem, Development of acetazolamide loaded bilosomes for improved ocular delivery: Preparation, characterization and in vivo evaluation. Journal of Drug Delivery Science and Technology, 2020. 59: p. 101910.
5. Qureshi, D., et al., Synthesis of novel poly (vinyl alcohol)/tamarind gum/bentonite-based composite films for drug delivery applications. Colloids and Surfaces A: Physicochemical and Engineering Aspects, 2021. 613: p. 126043.
6. Mašek, J., et al., Multi-layered nanofibrous mucoadhesive films for buccal and sublingual administration of drug-delivery and vaccination nanoparticles-important step towards effective mucosal vaccines. Journal of Controlled Release, 2017. 249: p. 183-195.
7. Boateng, J. and A. Popescu, Composite bi-layered erodible films for potential ocular drug delivery. Colloids and Surfaces B: Biointerfaces, 2016. 145: p. 353-361.
8. Abilova, G.K., et al., Chitosan/poly (2-ethyl-2-oxazoline) films for ocular drug delivery: Formulation, miscibility, in vitro and in vivo studies. European Polymer Journal, 2019. 116: p. 311-320.
9. Valencia-Gómez, L.E., et al., Chitosan/Mimosa tenuiflora films as potential cellular patch for skin regeneration. International journal of biological macromolecules, 2016. 93: p. 1217-1225.
10. Lai, K.L., et al., Orally-dissolving film for sublingual and buccal delivery of ropinirole. Colloids and Surfaces B: Biointerfaces, 2018. 163: p. 9-18.
11. R Badwaik, H., et al., Xanthan gum and its derivatives as a potential bio-polymeric carrier for drug delivery system. Current Drug Delivery, 2013. 10(5): p. 587-600.
12. Afshar, M., et al., Preparation and characterization of sodium alginate/polyvinyl alcohol hydrogel containing drug-loaded chitosan nanoparticles as a drug delivery system. Journal of Drug Delivery Science and Technology, 2020. 56: p. 101530.
13. Paolicelli, P., et al., effect of glycerol on the physical and mechanical properties of thin gellan gum films for oral drug delivery. International journal of pharmaceutics, 2018. 547(1-2): p. 226-234.
14. Kulikouskaya, V., et al., Physicochemical aspects of design of ultrathin films based on chitosan, pectin, and their silver nanocomposites with antiadhesive and bactericidal potential. Journal of Biomedical Materials Research Part A, 2022. 110(1): p. 217-228.
15. Cazón, P., M. Vázquez, and G. Velazquez, Novel composite films based on cellulose reinforced with chitosan and polyvinyl alcohol: Effect on mechanical properties and water vapour permeability. Polymer Testing, 2018. 69: p. 536-544.
16. Choo, K., et al., Preparation and characterization of polyvinyl alcohol-chitosan composite films reinforced with cellulose nanofiber. Materials, 2016. 9(8): p. 644.
17. Gajra*, B., et al., Poly vinyl alcohol hydrogel and its pharmaceutical and biomedical applications: A review. Int. J. Pharm. Res, 2012. 4: p. 2026.
18. Abdullah, Z.W. and Y. Dong, Biodegradable and water resistant poly (vinyl) alcohol (PVA)/starch (ST)/glycerol (GL)/halloysite nanotube (HNT) nanocomposite films for sustainable food packaging. Frontiers in materials, 2019: p. 58.
19. Aslam, M., M.A. Kalyar, and Z.A. Raza, Polyvinyl alcohol: A review of research status and use of polyvinyl alcohol based nanocomposites. Polymer Engineering & Science, 2018. 58(12): p. 2119-2132.
20. Kumar, A. and S.S. Han, PVA-based hydrogels for tissue engineering: A review. International journal of polymeric materials and polymeric biomaterials, 2017. 66(4): p. 159-182.
21. Kamoun, E.A., E.-R.S. Kenawy, and X. Chen, A review on polymeric hydrogel membranes for wound dressing applications: PVA-based hydrogel dressings. Journal of advanced research, 2017. 8(3): p. 217-233.
22. Gaaz, T.S., et al., Properties and applications of polyvinyl alcohol, halloysite nanotubes and their nanocomposites. Molecules, 2015. 20(12): p. 22833-22847.
23. Halima, NB, Poly (vinyl alcohol): review of its promising applications and insights into biodegradation. RSC advances, 2016. 6(46): p. 39823-39832.

24. Silva, M.M., et al., Lime-based restoration paints: characterization and evaluation of formulations using a native species from the Amazon flora and PVA-based glue as additives. Ambiente Construído, 2017. 17: p. 7-23.
25. Liu, J.-C. and K.H. Tan, Fire resistance of strain hardening cementitious composite with hybrid PVA and steel fibers. Construction and Building Materials, 2017. 135: p. 600-611.
26. Khoerunnisa, F., Y. Sonjaya, and N. Chotimah, Physical and chemical characteristics of alginate-poly (vinyl alcohol) based controlled release hydrogel. Journal of Environmental Chemical Engineering, 2016. 4(4): p. 4863-4869.
27. Fan, L., et al., Preparation and characterization of chitosan/gelatin/PVA hydrogel for wound dressings. Carbohydrate polymers, 2016. 146: p. 427-434.
28. Morandim-Giannetti, A.d.A., et al., Characterization of PVA/glutaraldehyde hydrogels obtained using Central Composite Rotatable Design (CCRD). Journal of Biomedical Materials Research Part B: Applied Biomaterials, 2018. 106(4): p. 1558-1566.
29. Ma, Q., et al., Rheology of film-forming solutions and physical properties of tara gum film reinforced with polyvinyl alcohol (PVA). Food Hydrocolloids, 2017. 63: p. 677-684.
30. Lan, W., et al., Ultraflexible transparent film heater made of Ag nanowire/PVA composite for rapid-response thermotherapy pads. ACS applied materials & interfaces, 2017. 9(7): p. 6644-6651.
31. Barreiros, Y., et al., Xanthan gum-based film-forming suspension containing essential oils: Production and in vitro antimicrobial activity evaluation against mastitis-causing microorganisms. LWT, 2022. 153: p. 112470.
32. Mukerabigwi, J.F., et al., Urea fertilizer coated with biodegradable polymers and diatomite for slow release and water retention. Journal of Coatings Technology and Research, 2015. 12(6): p. 1085-1094.
33. Jana, S., et al., Gellan gum (GG)-based IPN microbeads for sustained drug release. Journal of Drug Delivery Science and Technology, 2022. 69: p. 103034.
34. Destruel, P.-L., et al., Novel in situ gelling ophthalmic drug delivery system based on gellan gum and hydroxyethylcellulose: Innovative rheological characterization, in vitro and in vivo evidence of a sustained precorneal retention time. International Journal of Pharmaceutics, 2020. 574: p. 118734.
35. Munarin, F., M.C. Tanzi, and P. Petrini, Advances in biomedical applications of pectin gels. International journal of biological macromolecules, 2012. 51(4): p. 681-689.
36. Jain, D. and D. Bar-Shalom, Alginate drug delivery systems: application in context of pharmaceutical and biomedical research. Drug development and industrial pharmacy, 2014. 40(12): p. 1576-1584.
37. Liew, C.V., et al., evaluation of sodium alginate as drug release modifier in matrix tablets. International journal of pharmaceutics, 2006. 309(1-2): p. 25-37.
38. Shastri, DH, L. Patel, and R. Parikh, Studies on in situ hydrogel: a smart way for safe and sustained ocular drug delivery. Journal of Young Pharmacists, 2010. 2(2): p. 116-120.
39. Singh, A. and A. Bali, Formulation and characterization of transdermal patches for controlled delivery of duloxetine hydrochloride. Journal of Analytical Science and Technology, 2016. 7(1): p. 1-13.
40. Fathalla, Z.M., et al., Poloxamer-based thermoresponsive ketorolac tromethamine in situ gel preparations: Design, characterisation, toxicity and transcorneal permeation studies. European Journal of Pharmaceutics and Biopharmaceutics, 2017. 114: p. 119-134.
41. Shah, D.K., et al., Development of olive oil based organogels using sorbitan monopalmitate and sorbitan monostearate: A comparative study. Journal of applied polymer science, 2013. 129(2): p. 793-805.
42. Suman, D.K., et al., Gelatin and rice starch-based phase-separated hydrogel formulations for controlled drug delivery applications, in Food, Medical, and Environmental Applications of Polysaccharides. 2021, Elsevier. p. 263-289.
43. Behera, KP, et al., Bentonite increases the corneal permeation of the drug from the tamarind gum hydrogels, in Food, Medical, and Environmental Applications of Polysaccharides. 2021, Elsevier. p. 291-322.
44. Mehra, N.K., et al., safety and toxicity of nanomaterials for ocular drug delivery applications. Nanotoxicology, 2016. 10(7): p. 836-860.
45. Yadav, I., et al., Synthesis and characterization of polyvinyl alcohol-carboxymethyl tamarind gum based composite films. Carbohydrate polymers, 2017. 165: p. 159-168.
46. Nandi, S., et al., Vildagliptin plasticized hydrogel film in the control of ocular inflammation after topical application: study of hydration and erosion behaviour. Zeitschrift für Physikalische Chemie, 2022. 236(2): p. 275-290.
47. Pal, K., A. Banthia, and D. Majumdar, Biomedical evaluation of polyvinyl alcohol–gelatin esterified hydrogel for wound dressing. Journal of Materials Science: Materials in Medicine, 2007. 18(9): p. 1889-1894.
48. Pal, K. and S. Pal, Development of porous hydroxyapatite scaffolds. Materials and manufacturing processes, 2006. 21(3): p. 325-328.
49. Rawooth, M., et al., Effect of Tamarind Gum on the Properties of Phase-Separated Poly (vinyl alcohol) Films. Polymers, 2022. 14(14): p. 2793.
50. Zhang, L., et al., Developing hydroxypropyl methylcellulose/hydroxypropyl starch blends for use as capsule materials. Carbohydrate Polymers, 2013. 98(1): p. 73-79.
51. Peng, X., et al., The Film-Forming Characterization and Structural Analysis of Pectin from Sunflower Heads. International Journal of Polymer Science, 2021. 2021.
52. Tomé, L.C., et al., Bioactive transparent films based on polysaccharides and cholinium carboxylate ionic liquids. Green Chemistry, 2015. 17(8): p. 4291-4299.
53. Aadil, K.R., et al., Investigation of poly (vinyl) alcohol-gellan gum based nanofiber as scaffolds for tissue engineering applications. Journal of Drug Delivery Science and Technology, 2019. 54: p. 101276.
54. Mishra, R.K., et al., Preparation and characterization of amidated pectin based hydrogels for drug delivery system. Journal of Materials Science: Materials in Medicine, 2008. 19(6): p. 2275-2280.
55. Zhong, C., et al., Flotation separation of scheelite and apatite by polysaccharide depressant xanthan gum. Minerals Engineering, 2021. 170: p. 107045.
56. Kacurakova, M., et al., FT-IR study of plant cell wall model compounds: pectic polysaccharides and hemicelluloses. Carbohydrate polymers, 2000. 43(2): p. 195-203.
57. Hao, Y.-M., Entrapment and release difference resulting from hydrogen bonding interactions in niosome. International journal of pharmaceutics, 2011. 403(1-2): p. 245-253.
58. Bharti, D., et al., Effect of Biodegradable Hydrophilic and Hydrophobic Emulsifiers on the Oleogels Containing Sunflower Wax and Sunflower Oil. Gels, 2021. 7(3): p. 133.
59. Paul, S.R., et al., Development of bigels based on stearic acid–rice bran oil oleogels and tamarind gum hydrogels for controlled delivery applications. Journal of Surfactants and Detergents, 2018. 21(1): p. 17-29.
60. Hazirah, M.N., M. Isa, and N. Sarbon, Effect of xanthan gum on the physical and mechanical properties of gelatin-carboxymethyl cellulose film blends. Food Packaging and Shelf Life, 2016. 9: p. 55-63.
61. Quereshi, D., et al., Neem seed oil and gum arabic-based oil-in-water emulsions as potential ocular drug delivery system. Journal of Dispersion Science and Technology, 2020. 41(13): p. 1911-1924.
62. Rawooth, M., et al., Synthesis and characterization of novel tamarind gum and rice bran oil-based emulgels for the ocular delivery of antibiotics. International Journal of Biological Macromolecules, 2020. 164: p. 1608-1620.